2002

Magnetic Measurements on Ga1-xMnxS in High Fields Using the Cantilever Technique

Carl W. Maymi
University of North Florida

Magnetic measurements on $Ga_{1-x}Mn_xS$ in high fields using the cantilever technique

Carl W. Maymi

Faculty Sponsor: Dr. Thomas M. Pekarek
Associate Professor of Physics

Abstract

High field magnetic measurements have been taken on the III-VI Diluted Magnetic Semiconductor $Ga_{1-x}Mn_xS$ at the National High Magnetic Field Laboratory. This paper discusses the calibration of magnetic measurements made using the cantilever technique. It has been discovered that efficiency of cantilevers may decline over time, signaled by the onset of an oscillatory effect in the cantilever data. (Feb. 2001)

Introduction

III-VI Diluted Magnetic Semiconductor Background

The new layered III-VI Diluted Magnetic Semiconductors (DMS) are 2-D systems containing transition metal ions (*e.g.* Mn, Fe, Co, *etc.*) in a III-VI semiconducting host (*e.g.* GaSe, GaS, *etc.*). The III-VI DMS $Ga_{1-x}Mn_xSe$ exhibits a strong red emission at 1.804 eV attributed to the Mn ions. The III-VI semiconductors are known for their remarkable nonlinear optical properties and are promising materials for photoelectronic applications. This work also complements the enormous progress in the II-VI DMS and the more recent efforts in the Mn doped III-V DMS systems.

Pekerak *et al* presented magnetization data on the III-VI DMS $Ga_{1-x}Mn_xSe$ that is strikingly different from any of the II-VI DMS data.[1] A key feature is a broad peak in the magnetization versus temperature data between 120 and 195 K that is ascribed to direct Mn-Mn pairs. This is a fundamentally different behavior that that observed in the heavily studied II-VI DMS. Except for this single publication, no previous magnetic or calorimetric measurements on III-VI DMS have been reported.

Since this presentation more recent work on the magnetic measurement on $Ga_{1-x}Mn_xS$ has been conducted.[2] Its magnetic behavior was remarkably different from $Ga_{1-x}Mn_xSe$ and II-VI DMS. The prominent broad peak between 120 and 195 K in the magnetization of $Ga_{1-x}Mn_xSe$, ascribed to direct Mn-Mn pairs, is absent in the $Ga_{1-x}Mn_xS$ data. This suggests that there are no direct Mn-Mn pairs in the GaS system. However, the magnetization of $Ga_{1-x}Mn_xS$ does show a sharp cusp at 11.3 K (an order of magnitude higher than the spin-glass transition in $Cd_{1-x}Mn_xS$) suggesting that a similar mechanism with Mn-Se-Mn pairs may be present in $Ga_{1-x}Mn_xS$. The exchange interactions in $Ga_{1-x}Mn_xSe$ and $Ga_{1-x}Mn_xS$ (with lower symmetry than the II-VI and III-V DMS) are more complex and exhibit significantly different magnetic properties. The magnetic and calorimetric measurements will provide key information for unraveling some of the observed novel magnetic effects.

The III-VI semiconductors GaSe, InSe, GaTe, and GaS have generated considerable interest in the last few years because they have remarkable nonlinear optical properties and are promising materials for photoelectronic applications in the visible range (the band gap for GaSe is 2.0 eV). Furthermore, Shigetomi *et al.*[3] and Lee *et al.*[4] studied Mn-doped GaSe samples and report a strong red emission at 1.804 eV (Fig. 1),[4] which is important for compatibility with commercial lasers. They attribute this emission line to the Mn ions' acceptor level. This makes $Ga_{1-x}Mn_xSe$ particularly interesting to study. Since the magnetic behavior is a measure of the field and temperature dependence of the Mn ion energy levels, the results of this work will lead to an increased understanding of this important emission line.

Figure 111. Generation mechanism of photoconductivity and photoluminescence in GaSe:Mn single crystals.
(This figure is based on Lee *et al.*).[4]

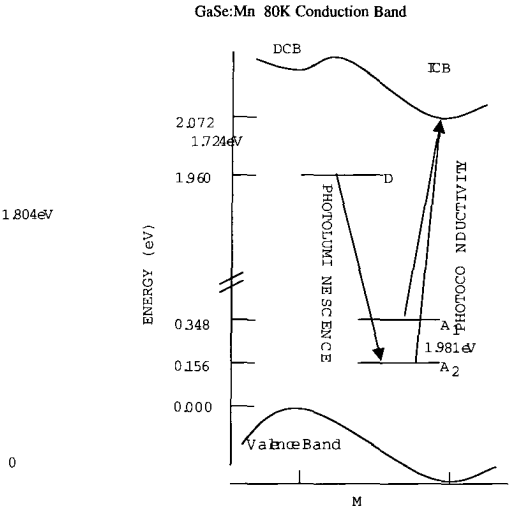

To understand the $Ga_{1-x}Mn_xS$ and other III-VI DMS completely enough to predict the behavior of these systems within a wide range of experimental conditions, it is essential to first know how the Mn ions behave individually as well as cooperatively throughout the crystal. Calorimetric and magnetic studies are well suited for this task.

Further investigation into the magnetic properties of $Ga_{1-x}Mn_xS$ are needed to determine the electronic levels of the individual Mn ions, the interactions of various nearest neighbor configurations (e.g. Mn-Mn, Mn-Se-Mn, Mn-Ga-Se-Mn, etc.), and the longer-range cooperative effects in the bulk crystal. This will directly provide information about how the temperature and field affect the electronic levels, in particular the levels giving rise to the 1.804 eV emission line in $Ga_{1-x}Mn_xSe$ (Fig.1).[4]

III-VI Semiconductors doped with Mn

There are only a few publications on Mn-doped GaSe including photoluminescence,[3,4] photoconductivity,[4] Hall effect,[3] electron spin resonance,[5,6] and deep-level transient spectroscopy measurements.[3] We have found no reported work on magnetic or calorimetric properties of III-VI DMS. The two early brief papers of electron spin resonance measurements on GaSe:Mn by Ishchenko *et al.*(1975)[6] and Konovalov *et al.*(1980)[5] show that the manganese goes in substitutionally as Mn^{2+} and established that the epsilon phase is common in these crystals. In 1986, Lee *et al.*4 established the energy diagram for the 1.804 eV photoluminescence line as well as the photoconductivity lines in GaSe:Mn (Fig. 1).

Figure 2: Crystal structure for $Ga_{1-x}Mn_xS$ and $Ga_{1-x}Mn_xSe$. The large solid circles are the Ga lattice sites in GaSe or the substitutional Mn lattice sites in $Ga_{1-x}Mn_xS$ or $Ga_{1-x}Mn_xSe$. The small squares are the S (or Se) lattice sites. Figure (a) shows a cross section of a four atom thick layer. The tetrahedral environment of the Ga or Mn lattice sites is emphasized with three neighboring S (or Se) ions as well as another Ga or Mn ion. A direct Mn-Mn bond is shown by the bold dotted line. The bold solid line emphasizes the bonds in a Mn-S-Mn pair. A Mn-Ga-S-Mn pair can be seen where the bold dotted line is the bond between the Ga and the first Mn ions and the bold solid lines then completes the Ga-S-Mn bonds.

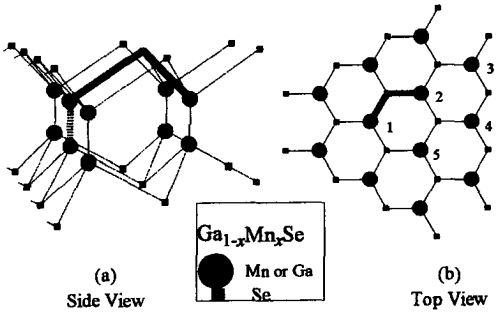

The work of Shigetomi *et al.*[3] in 1994 confirms the results of Lee *et al.*[4] and provides Hall effect and deep-level transient spectroscopy measurements confirming the 0.34 eV acceptor level. The results of the proposed magnetic and calorimetric investigations should provide additional insight into the published data reported in these papers.

Published Magnetic Measurements on $Ga_{1-x}Mn_xSe$

A key feature of $Ga_{1-x}Mn_xSe$ is its two-dimensional crystal structure. Each $Ga_{1-x}Mn_xSe$ layer is comprised of a top two-dimensional layer of Se ions, two middle layers of Ga ions, and a bottom layer of Se ions (Fig. 2). Within each four atom thick layer the bonding is covalent. Layers are weakly coupled through van der Waals bonding similar to mica, which further enhances the two-dimensional nature of this crystal. This is therefore an excellent system to investigate 2-D magnetism as well as the dimensional cross over between the 2-D and 3-D regimes.

Magnetic Measurements on $Ga_{1-x}Mn_xS$

We have already conducted initial magnetic measurements on single crystalline $Ga_{1-x}Mn_xS$. Magnetic versus temperature measurements taken in a 0.0050 and 0.1 T field are shown in figure 3. The prominent broad peak from 119 to 195 K in the magnetization of $Ga_{1-x}Mn_xSe$, ascribed to direct Mn-Mn pairs, is absent in our $Ga_{1-x}Mn_xS$ data. This suggests there are no direct Mn-Mn pairs in the $Ga_{1-x}Mn_xS$ system.

We see a prominent cusp at 11.3 K in figure 4. While the presence of a cusp of this sort can arise from several different mechanisms including a spin-glass transition or cluster locking, many of the II-VI DMS also display similar cusps at low temperature due (in the case of the II-VI DMS) to a spin-glass transition. However, a more sophisticated analysis is needed before any specific conclusions can be drawn from the presence of the cusp in our $Ga_{1-x}Mn_xS$ data. Nonetheless, the presence of the cusp provides additional evidence to the Curie-Weiss behavior that there are Mn-Se-Mn (and/or perhaps Mn-Se-Ga-Mn) pairs in $Ga_{1-x}Mn_xS$.

Figure. 3: Magnetization versus temperature data for $Ga_{1-x}Mn_xS$ in a 0.0050 and 0.1 T field are shown by solid circles. The complex structure ascribed to direct Mn-Mn pairs in the $Ga_{1-x}Mn_xSe$ data is completely missing through the entire range in field. This suggests there are no direct Mn-Mn pairs in the GaS system.

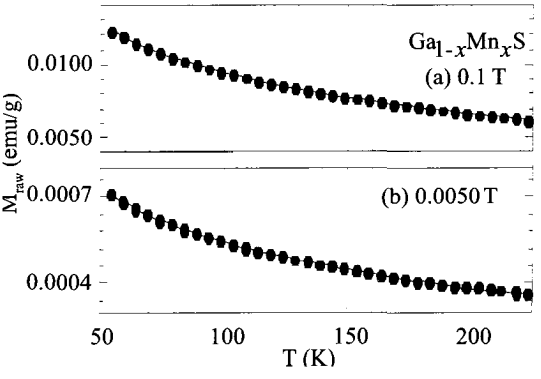

Figure 4. Magnetization versus temperature for $Ga_{1-x}Mn_xS$ in a 0.0050 and 0.1 T field are shown by solid circles. The cusp at 11.3 K is reminiscent of a spin-glass transition in many of the II-VI DMS.

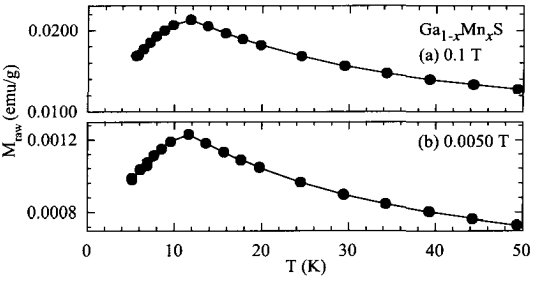

The absence of the peak in figure 3, the Curie-Weiss behavior (not shown), and now the cusp in figure 4 all are reminiscent of the II-VI DMS in stark contrast to the dramatically different behavior of $Ga_{1-x}Mn_xSe$. Still there are some features of the $Ga_{1-x}Mn_xS$ data that distinguish

$Ga_{1-x}Mn_xS$ from the II-VI DMS. For one, the cusp we observe at 11.3 K is more than an order of magnitude higher than the spin-glass transition in $Cd_{0.934}Mn_{0.066}S$, which occurs at ~0.08 K.

The singlet behavior of isolated Mn ions in $Ga_{1-x}Mn_xS$ is also somewhat unusual compared with the II-VI DMS. At 10 K in a 6 T field (not shown), the magnetization for an $x = 0.066$ sample has reached ~10% of the expected saturation magnetization for $S = 5/2$ and remains roughly linear with field where $M/H = 2 \times 10^{-5}$ emu/g G. This linear response is dramatically different from the behavior of V, Cr, Co, and Mn-based II-VI DMS, which all show definite signs of saturation by 6 T at 10 K. However, Fe-based II-VI DMS exhibit Van Vleck paramagnetism with an initially weak linear response. It is still too soon to conclude that singlet Mn ions in $Ga_{1-x}Mn_xS$ and $Ga_{1-x}Mn_xSe$ are Van Vleck paramagnets. The difference between the $Ga_{1-x}Mn_xSe$ and $Ga_{1-x}Mn_xS$ systems may provide a good opportunity to investigate the difference in exchange channels between Mn-Mn versus Mn-Se-Mn pairs and the different magnetic behavior each consequently exhibits.

Cantilever Magnetometry

Magnetization measurements were conducted at the National High Magnetic Field Laboratory (NHMFL) in Tallahassee, FL. The NHMFL is one of only nine such facilities in the world and is the largest and high-powered magnet laboratory of it's kind. Magnetization measurements were performed using a newly developed cantilever technique. This process involves mounting a ~0.0010g sample on the cantilever device at the end of a probe (Figure 5). The cantilever device consists of a cantilever beam; where the sample is attached, placed into the helium-3 cryostat, and cooled. The probe was then lowered into a NHMFL 30 Tesla resistive magnet.

Cantilever magnetometry is based on the principle that a magnetic sample secured to the flexible beam will encounter a torque and a force when placed in an external magnetic field. Magnetization M is the magnetic dipole moment per unit volume of the sample. Magnetic moments experience a torque

$$t = M \times B \qquad (1)$$

in the presence of a uniform magnetic field B. This allows us to find the component of magnetization perpendicular to the applied field. A force

$$F = M \cdot {}^{dB}/_{dz} \qquad (2)$$

is exerted on a magnetic moment in a field gradient. This force allows us to measure to the magnetization component parallel to the applied field. The cantilever beam responds by a deflection proportional to the torque or force on the sample. The deflection of the cantilever beam is measured by a change in capacitance between the fixed base plate and the flexible cantilever beam, which holds the sample (Fig.1). Measurement of the capacitance is made with a 1616 General Radio capacitance bridge and a lock-in amplifier used to drive the bridge and detect the imbalance signal.[7] Theoretically, it is possible to obtain calibrated magnetization curves from this technique. Relative measurements are easily obtained.[7] In the case of Ga_{1-x} Mn_x S, the perpendicular signal was small compared to the parallel magnetization. Therefore, we will focus on the parallel magnetization of Ga_{1-x} Mn_x S.

Calibration

Our most recent magnet time at the NHMFL has provided a chance to improve the calibration techniques for cantilever magnetometry. Measurements taken at NHMFL give the raw data for magnetization measurements in terms of voltage V versus applied field H. The following section is devoted to describing the calibration method used to convert the raw voltage data into calibrated magnetization (emu/g) data.

A small wire loop attached to the surface of our cantilever. By setting a current in this loop, we generate a known magnetic dipole moment. In a magnetic field gradient, this magnetic dipole produces a force on the cantilever. The force deflects the cantilever and changes the capacitance. By supplying a known current to the loop of known area we can calculate the current loops magnetic dipole moment, the force exerted on the cantilever beam, and the corresponding change in capacitance for such a force. From this we may determine a relationship between the voltages given in the data file and the magnetization of the sample. The following is a detailed description of the calibration process.

To begin the calibration procedure, place the probe above the magnet center where it will be in the maximum field gradient when the magnetic field B_{SetCal} is set. Set the temperature and wait for it to stabilize. The area of the current loop should be recorded. The setting of the capacitance bridge should be recorded as well as the lock-in signal in zero field.

Set the current I_{Loop} and record both the values of the set current and the resulting change in capacitance ΔC from the zero current value.

The raw data files record a voltage data point V_{Data}. This voltage comes from the lock-in amplifier that is used to drive the capacitance bridge and detect the imbalance signal. For the calibration, the relationship between a change in capacitance and a change in voltage must be established. This is done at the NHMFL by making changes in the capacitance bridge by hand and noting the change in voltage from the lock-in. This should be done several times with the applied field B_{SetCal} and temperature held constant. When completed, the conversion coefficient $^{\Delta C}/_{\Delta V}$ will be used to convert the raw voltage data to a capacitance.
The magnetic dipole moment of the loop is given by:

$$M_{Loop} = A_{Loop}\, I_{Loop} \qquad (3)$$

Recall from $F = M \cdot {}^{dB}/_{dz}$ that the force F_{Loop} exerted on the loop is given by:

$$F_{Loop} = M_{Loop} \cdot ({}^{dB}/_{dz})_{Cal}$$
$$F_{Loop} = (A_{Loop}\, I_{Loop}) \cdot ({}^{dB}/_{dz})_{Cal} \qquad (4)$$

where $({}^{dB}/_{dz})_{Cal}$ is the field gradient when the constant applied field is set during the calibration procedure itself.
The sample on the cantilever also produces a force

$$F_{Sample} = M_{II} \cdot ({}^{dB}/_{dz})_{Data} \qquad (5)$$

where $({}^{dB}/_{dz})_{Data}$ is the constantly changing field gradient during a normal data sweep.

Using the change in capacitance ΔC found when a current is supplied in the loop, the conversion coefficient $^{\Delta C}/_{\Delta V}$, and the voltage data point V_{Data}, we get:

$$F_{Sample} = (V_{Data})\ ({}^{\Delta C}/_{\Delta V})\ ((F_{Loop})/(\Delta C)) \qquad (6)$$

M_{II} is the final value we seek so, solving for M_{II} in (5) and substituting (6) for F_{Sample}

$$M_{II} = [(V_{Data})\ ({}^{\Delta C}/_{\Delta V})\ ((F_{Loop})/(\Delta C))]\ /\ ({}^{dB}/_{dz})_{Data} \qquad (7)$$
$$M_{II} = [(V_{Data})\ ({}^{\Delta C}/_{\Delta V})\ ((A_{Loop}\, I_{Loop}\ ({}^{dB}/_{dz})_{Cal})/(\Delta C))]\ /\ ({}^{dB}/_{dz})_{Data} \qquad (8)$$

We now must determine the values of the two different field gradients in the numerator and denominator. Each cell containing a magnet at the NHMFL has it's own Magnet Profile from which the value of the field and field gradient may be found for any position inside the magnet core. The value of the applied field at 8 cm up from center is found with the following equation.

$$B_{8cm\ up} = B_{set}\ (B_{max\ 8cm\ up} / B_{max\ center}) \qquad (9)$$

$B_{max\ 8cm\ up} / B_{max\ center}$ is given in the magnet profile. The maximum field gradient of the 30 T magnet in Cell 9 is found at 8 cm up from center. This point may differ with the

use of different magnets in different cells at the NHMFL. The field gradient can also be found using the Magnet Profile. The following equation gives the value of the field gradient.

$$^{dB}/_{dz} = B_{set}\,[(B_{max\ 8cm\ up} / B_{max\ center})\,((B_{max\ center})^{-1}\,(^{dB}/_{dz})_{8cm\ up})] \qquad (10)$$

Note that the difference between the field gradients in equation 8 lies in the value of B_{set} in equation 10. The field gradient $(^{dB}/_{dz})_{Cal}$ in the numerator comes from the calibration procedure where B_{SetCal} is a constant value. On the other hand, the field gradient $(^{dB}/_{dz})_{Data}$ in the denominator is found by using the ever changing value of B_{set} as the magnetic field is ramped up and down through the data run. Use B_{Data} to represent the changing applied field of the data runs, the second term of equation 10 cancels out in equation 8 and we are left with:

$$M_{II} = [(V_{Data}) / (B_{Data})]\ [(^{\Delta C}/_{\Delta V})\,((A_{Loop}\,I_{Loop}\,B_{SetCal})/(\Delta C))] \qquad (11)$$

All values in the second term are known. We may set this term equal to a calibration constant $C_{Cantilever}$.

$$M_{II} = [(V_{Data}) / (B_{Data})]\ C_{Cantilever}\ ;\quad C_{Cantilever} = [(^{\Delta C}/_{\Delta V})\,((A_{Loop}\,I_{Loop}\,B_{SetCal})/(\Delta C) \qquad (12)$$

Both V_{Data} and B_{Data} are extracted from the raw data files.

Note that this M_{II} value is given in units of J/T or Am^2. We seek a final value with the units of emu/g. 1 J/T is equivalent to 10^{-3} emu. Simple of use this conversion and dividing by the mass of the sample we arrive at units of emu/g.

Figure 5. General Schematic of the cantilever used at the Nationsl High Magnetic Field Laboratory.

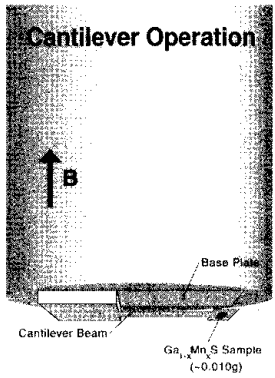

Figure 6. Magnetization versus magnetic field data. Oscillations and the hysteretical nature of the curve suggests a faulty cantilever.

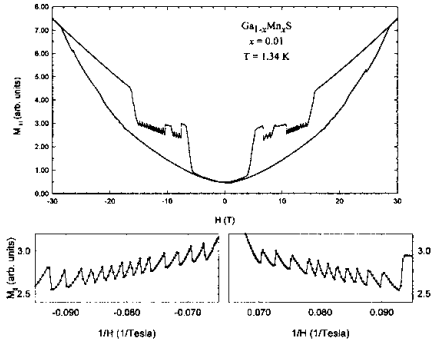

Cantilever effect

Recent measurements made using the cantilever method at the National High Magnetic Field Laboratory have shown an oscillatory and hysteretical effect in the magnetization as a function of field (Figure 6). Preliminary analysis suggested that these oscillations may have been due to the de Haas-van Alphen effect. The oscillations are observed at very low temperatures and high magnetic fields. The oscillations in our $Ga_{1-x}Mn_xS$ sample occur in the temperature range of 1.3K -1.7K and field range of 8T -18T.

After several attempts to identify the source of these oscillations, it has been found that the mechanical properties of the

cantilever declines over time. The decline of a cantilever's usefulness is signaled by the onset of an oscillatory and hysteresis effect in the cantilever data. Our research group has played an important role in identifying this effect. This information will aid future NHMFL magnet users to quickly identify the source of faulty data; saving both time and money.

Calibrated results for magnetic measurement on $Ga_{1-x}Mn_xS$ in high magnetic fields using the cantilever tenchnique

The following pages show our results for the calibrated magnetization measurements on $Ga_{1-x}Mn_xS$. Current theoretical work is in the final stages and will be submitted for publication along with this data in an appropriate peer-reviewed journal.

Appendix A

The following is an example of a SigmaPlot transform used to calibrate raw cantilever data from the NHMFL.

```
;P1252ML4b_001

;PARAMETERS
cell(11,1) = "sample mass (g )="
cell(12,1) = mass
mass = 0.0023

cell(11,2) = "I_Loop (A )="
cell(12,2) = I_Loop
I_Loop = 10e-3

cell(11,3) = "A_Loop (m*m)="
cell(12,3) = A_Loop
A_Loop = 1.295907e-5
cell(11,4) = "deltaC/deltaV (F/V)="
cell(12,4) = CV
CV = 6.2696e-10

cell(11,5) = "deltaC_5K (F)="
cell(12,5) = deltaC
deltaC = 0.000365e-12

cell(11,6) = "B/B_o ="
cell(12,6) = BB_o
BB_o = .79

; corect B_set to B at the sample 8cm up
col(13) = col(1) * BB_o

;calibrate data
cell(11,7) = "cal const , K="
cell(12,7) = K
K = (CV * ((I_Loop * A_Loop *
5)/deltaC)) * 1e3
col(14) = Mag_II
Mag_II = -(col(3)/col(1) * K)/mass
```

Appendix B

ΔC = change in capacitance when a current is placed in the loop

A_{Loop} = area of the loop
I_{Loop} = current in the loop
B_{SetCal} = applied field value while performing the initial calibration procedures
$^{\Delta C}/_{\Delta V}$ = conversion coefficient used to convert the raw voltage data to a capacitance
M_{Loop} = magnetic dipole moment of the loop
$(^{dB}/_{dz})_{Cal}$ = field gradient value while performing the initial calibration procedures
F_{Loop} = force on the loop in a field gradient
F_{Sample} = force on the sample in a field gradient
M_{II} = magnetization of the sample
$(^{dB}/_{dz})_{Data}$ = changing field gradient value during data sweeps
V_{Data} = raw voltage data point value

$$F_{Sample} = (V_{Data})\ (^{\Delta C}/_{\Delta V})\ ((F_{Loop})/(\Delta C)) \qquad (6)$$

$B_{8cm\ up}$ = actual field value at maximum field gradient
B_{set} = set field value

Field (B_{SetCal})	Current Loop (I_{loop})	Capacitance Bridge Value
5T	+10mA	.98625pF
	0mA	.98659pF
	-10mA	.98698pF
10T	+10mA	.98305pF
	0mA	.98378pF
	-10mA	.98456pF
15T	+10mA	.97874pF
	0mA	.97994pF
	-10mA	.98096pF

($B_{max\ 8cm\ up}$ / $B_{max\ center}$) = given in the magnet profile

$C_{Cantilever}$ = calibration coeficient

The following is a step by step example of the calibration of a single raw data point. After following the calibration procedure at the NHMFL as described above, the following values are given.

Data from the initial calibration steps would appear as follows.

Capacitance Bridge Value	Lock-in Value
-7.32microV	.98456pF
-24.90microV	.99556pF
+38.90microV	.95556pF

Using the calibration data at 5T, the following values are found:

ΔC = .000365E-12 F

A_{Loop} = 6.25E-6 m^2

I_{Loop} = 10^{-3} A

B_{SetCal} = 5 T

$\Delta C/\Delta V$ = 6.2695925E-10 F/V

mass = 0.0023g

The calibration coefficient can be found using equation 12

$C_{Cantilever}$ = .53678 J/T

or in units of emu/g

$C_{Cantilever}$ = 233382 emu/g

This value can then be used as the calibration coefficient in a math transform similar to that shown in Appendix A.

Work Cited

[1] T. M. Pekarek, B. C. Crooker, I. Miotkowski, and A. K. Ramdas, J. Appl. Phys. 83, 6557 (1998).

[2] T. M. Pekarek, M. Duffy, J. Garner, B. C. Crooker, I. Miotkowski, and A. K. Ramdas, J. Appl. Phys. 87, 6448 (2000).

[3] S. Shigetomi, T. Ikari, H. Nakashima, J. Appl. Phys. 76, 310 (1994).

[4] S. Lee, S. Hahn, C. Chung, S. Yun, and W. Kim, Solid State Commun. 60, 453 (1986).

[5] V. I. Konovalov, S. S. Ishchenko, and S. M. Okulov, Sov. Phys. Solid State 22, 1070 (1980).

[6] S. S. Ishchenko, S. M. Okulov, G. B. Abdullaev, G. L. Belen'kii, V. G. Grachev, M. F. Deigen, R. Kh. Nani. E. Yu. Salaev, and Yu. G. Samenov, Sov. Phys. Solid State 17, 1168 (1975).

[7] Donavan Hall, Magnetic Measurements with Metal Film Cantilevers: A user's Guide (1999)